

Influence of Different Polymers on the Crystallization Tendency of Molecularly Dispersed Amorphous Felodipine

HAJIME KONNO, LYNNE S. TAYLOR

Department of Industrial and Physical Pharmacy, School of Pharmacy, Purdue University, West Lafayette, Indiana 47907

Received 2 February 2006; revised 3 April 2006; accepted 11 May 2006

Published online in Wiley InterScience (www.interscience.wiley.com). DOI 10.1002/jps.20697

ABSTRACT: The ability of various polymers to inhibit the crystallization of amorphous felodipine was studied in amorphous molecular dispersions. Spin-coated films of felodipine with poly(vinylpyrrolidone) (PVP), hydroxypropylmethylcellulose acetate succinate (HPMCAS), and hydroxypropylmethylcellulose (HPMC) were prepared and used for measurement of the nucleation rate and to probe drug–polymer intermolecular interactions. Bulk solid dispersions were prepared by a solvent evaporation method and characterized using thermal analysis. It was found that each polymer was able to significantly decrease the nucleation rate of amorphous felodipine even at low concentrations (3–25% w/w). Each polymer was found to affect the nucleation rate to a similar extent at an equivalent weight fraction. For HPMC and HPMCAS, thermal analysis indicated that the glass transition temperature (T_g) of the solid dispersions were not significantly different from that of felodipine alone, whereas an increase in T_g was observed for the PVP containing solid dispersions. Infrared spectroscopic studies indicated that hydrogen bonding interactions were formed between felodipine and each of the polymers. These interactions were stronger between felodipine and PVP than for the other polymers. It was speculated that, at the concentrations employed, the polymers reduce the nucleation rate through increasing the kinetic barrier to nucleation. © 2006 Wiley-Liss, Inc. and the American Pharmacists Association *J Pharm Sci* 95:2692–2705, 2006

Keywords: solid dispersion; amorphous; crystallization; calorimetry (DSC); FTIR

INTRODUCTION

It is well recognized that using the amorphous form of a drug can be a useful approach to improve the dissolution behavior and bioavailability of poorly water-soluble drugs. However, amorphous compounds are thermodynamically unstable and may recrystallize during storage negating the dissolution improvement for poorly water-

soluble drugs. Consequently, many researchers have attempted to stabilize amorphous compounds through the formation of solid dispersions¹ and this topic has been the subject of several reviews.^{2–5} Solid dispersions are typically formulated by combining the active ingredient with a carrier and the properties of each component will influence the physicochemical properties of the resultant solid dispersion. Water-soluble synthetic polymers such as poly(vinylpyrrolidone) (PVP)^{6–8} and polyethylene glycol (PEG)^{9–11} have been extensively investigated as carriers for solid dispersions, as have the cellulose analogues, for example, hydroxypropylmethylcellulose (HPMC).^{12,13}

Based on studies of crystallization from the amorphous state, the glass transition temperature

Hajime Konno's present address is Astellas Pharma Inc., 2-1-6 Kashima, Yodogawa-ku, Osaka 532-8514, Japan.

Correspondence to: Lynne S. Taylor (Telephone: +1-765-496-6614; Fax: +1-765-494-6545; E-mail: ltaylor@pharmacy.purdue.edu)

Journal of Pharmaceutical Sciences, Vol. 95, 2692–2705 (2006)
© 2006 Wiley-Liss, Inc. and the American Pharmacists Association

(T_g) is considered to be a key parameter since it delineates a temperature range between high and low molecular mobility.¹⁴ Thus, the stabilizing effect of polymers possessing a high T_g relative to the T_g of the drug has been attributed to their antiplasticizing effect.^{15,16} However, it should be noted that several studies have shown that significant crystallization occurs well below the T_g ^{17,18} and it has also been reported that polymers can stabilize against crystallization even when the T_g of the system is not increased.

Interactions between drug compounds and polymers in solid dispersions are also thought to contribute to the stabilization of amorphous drug compounds. Several studies have shown the formation of ion–dipole interactions, intermolecular hydrogen bonding between drug and polymer and the disruption of the hydrogen bonding pattern characteristic to the crystalline structure.^{19–21} Conversely, other studies have shown stabilization in systems where hydrogen bonding interactions are not possible due to the chemistry of the system, so clearly hydrogen bonding *per se* is not a specific prerequisite.¹⁵

Based on the preceding discussion, it is apparent that the physicochemical properties of polymers necessary to inhibit crystallization from the amorphous state are not fully understood. The purpose of this study was to investigate the ability of three different polymers, PVP, HPMC, and hydroxypropylmethylcellulose acetate succinate (HPMCAS) to stabilize a model amorphous compound, felodipine, against crystallization. These polymers have different glass transition temperatures and vary in the ability to interact with the model compound due to variations in functional groups capable of hydrogen bonding. The influence of each polymer on the nucleation rate of the drug, in the absence of any moisture, was measured in thin, optically transparent films prepared by spin coating. Differential

scanning calorimetry (DSC) and infrared (IR) spectroscopy were used to characterize the solid dispersions.

MATERIALS

Felodipine was generous gift from AstraZeneca, Södertälje, Sweden. Poly(vinylpyrrolidone) K29/32 (PVP) was purchased from Sigma-Aldrich Co., St. Louis, MO. Hydroxypropylmethylcellulose acetate succinate (HPMCAS: Shin-Etsu AQOAT[®], Type AS-MF) and hydroxypropylmethylcellulose USP (HPMC: Pharmacoat[®] type 606) were generous gifts from Shin-Etsu Chemical Co., Niigata, Japan. Further information about the polymers is shown in Table 1. Dichloromethane and ethanol were obtained from Mallinckrodt Baker, Inc., Paris, KY and Aaper Alcohol and Chemical Co., Shelbyville, KY, respectively.

METHODS

Preparation of Spin-Coated Films

For the analysis of nucleation rate and IR measurement, samples were prepared by spin-coating method. The spin-coating operations were performed using spin-coater KW-4A (Chemat Technology, Inc., Northridge, CA). Felodipine and polymer were dissolved together in a mixed solvent (dichloromethane: ethanol = 1:1), and then the solution was dropped onto a clean substrate spinning at about 2500 rpm. During spinning, the solute spread out onto the substrate and the solvent was evaporated. The thin film obtained was heated to 90°C for several minutes to remove residual solvent from the film. The preparation was performed under dry conditions (glove box purged with N₂ gas, RH < 10%) to minimize contact with water vapor.

Table 1. Summary of Polymer Characteristics

	MW	Average MW of side chain	Number of functional groups per monomer
PVP	58000	111	Pyrrolidone, 1.0
HPMCAS	18000	252	Methoxyl, 1.9; acetyl, 0.5
HPMC	35600	202	Hydroxypropyl, 0.2; succinoyl, 0.3 Methoxyl, 1.9; hydroxypropyl, 0.2

The information about HPMCAS and HPMC was provided by Shinetsu Chemical Co, Ltd., Niigata, Japan.

Evaluation of Nucleation Sites with Microscopic Observation

For the evaluation of nucleation rate, spin-coated films were prepared on glass cover slips. The spin-coated samples were stored in desiccators over phosphorus pentoxide (0% RH) at 22°C. The samples were removed from the desiccators for microscopic observation. At the end of the evaluation (approximately 5 min) they were returned to the desiccators until the next sampling time, when the same samples were used again.

The number of nucleation sites was determined using polarized light microscopy, Olympus BHS system microscope (Olympus Co., Tokyo, Japan). A total of 12 individual areas were observed for every sample at each time point in order to measure the number of nucleation sites. The site number of density per unit volume was calculated by multiplying the site number density per unit area,²² by the depth of field of the appropriate lens. The depth of field (D_{tot}) as a function of the wavelength of the light used ($\lambda = 550$ nm) and the numerical aperture (NA) of the lens is given in the following equation.²³

$$D_{\text{tot}} = \frac{\lambda n}{\text{NA}^2} + \frac{n \cdot e}{M \cdot \text{NA}} \quad (1)$$

Where n is the refractive index of the medium ($n_{\text{air}} = 1.000$), e is the smallest distance that can be resolved by a detector ($e = 14$ μm), and M is lateral magnification ($M = 10\times$). Based on these calculations, the D_{tot} in this study was 0.0144 mm for 10 \times objective.

In some cases preferential nucleation and growth appeared at the periphery of the films but these sites were not included in our analysis. Triplicate experiments were performed using the procedure described above.

Thermal Analysis

For thermal analysis, samples were prepared using a vacuum drying technique. Felodipine and polymer were dissolved together in a mixed solvent (dichloromethane: ethanol = 1:1), and then the solvent was removed using a rotary evaporator immersed in a water bath held at 60°C. In order to remove residual solvent, the sample was left under vacuum for several hours.

DSC measurements were performed on a TA 2920 modulated DSC (TA Instruments, New

Castle, DE). Indium and benzophenone were used to calibrate the temperature scale and indium was used to calibrate the enthalpic response. Water and indium were subsequently run as samples in order to confirm the temperature calibration. The onset of melting for these samples was within 0.5°C of the expected values.

Approximately 5 mg of the sample was weighed into an aluminum sample pan (Perkin Elmer, Boston, MA) and then hermetically sealed. The glass transition temperature (T_g) was determined at a heating rate of 20 K/min, and the onset temperature was reported. All values of the T_g were determined from the second scan after heating the sample to 20 K above T_g in order to erase the previous thermal history. Repeated temperature cycling above and below T_g did not change the value obtained suggesting that the samples were miscible. Experiments were performed in triplicate.

The T_g values of solid dispersions were predicted using the Gordon–Taylor equation which assumes that two components are miscible and that the free volumes of the components are additive.²⁴ The T_g of mixture, T_{g12} , is defined as

$$T_{g12} = \frac{w_1 T_{g1} + K w_2 T_{g2}}{w_1 + K w_2} \quad (2)$$

where w_1 and w_2 are the weight fractions of each component, T_{g1} and T_{g2} are the respective glass transition temperatures. The constant K is calculated from the ratio of the density of each component (ρ) and the T_g of the two components.^{24,25}

$$K = \frac{T_{g1} \rho_1}{T_{g2} \rho_2} \quad (3)$$

Densities for PVP and amorphous felodipine were measured using helium pycnometry and were 1.25 and 1.33 g/cm³, respectively. Values of 1.29 and 1.19 g/cm³ were used for HPMCAS and HPMC respectively and were supplied by the manufacturer.

The Couchman–Karasz model can also be used to predict the T_g values of solid dispersions.²⁶ The Couchman–Karasz equation takes the same form as Equation 2, but K is defined as

$$K = \frac{\Delta C_{p1}}{\Delta C_{p2}} \quad (4)$$

where ΔC_p is the change in specific heat capacity at the T_g of each component. The ΔC_p values measured were: 0.33 J/g/K (felodipine), 0.20 J/g/K

(PVP), 0.31 J/g/K (HPMCAS), and 0.25 J/g/K (HPMC).

For the enthalpy relaxation measurements, amorphous felodipine:polymer (9:1 w/w ratio) solid dispersions were prepared in a similar manner as described above. Samples were stored for 0–38 h at 2°C (approximately 40°C below the T_g). This temperature was chosen to avoid crystallization. After cooling to –20°C, the samples were heated at 20°C/min and the endothermic recovery was measured. Crystallization of felodipine was not observed during the enthalpy relaxation measurement, as indicated by the absence of a melting peak for felodipine.

The fraction of glass relaxed at time t , $\phi(t)$, was calculated using Equation (5):²⁷

$$\phi(t) = \frac{\Delta H_t}{\Delta H_\infty} \quad (5)$$

where ΔH_t is the enthalpy recovery at time t , and ΔH_∞ is the maximum enthalpy recovery calculated from ΔC_p according to Equation (6)

$$\Delta H_\infty = \Delta C_p \times (T_g - T_a) \quad (6)$$

where T_a is the aging temperature. T_g and ΔC_p values observed for the sample prior to storage were used to calculate the ΔH_∞ value. The average relaxation times, τ , calculated according to the Kohlrausch–Williams–Watts equation [Eq. (7)]^{21,27,28}

$$1 - \phi(t) = \exp \left[\left(\frac{-t}{\tau} \right)^\beta \right] \quad (7)$$

where β is a parameter representing the distribution of the relaxation times.

Infrared Spectroscopy

For FT-IR measurements, spin-coated samples were prepared on ZnS discs in a glove box purged with dry N₂ using a method similar to that described for the preparation of the microscopy samples. Samples prepared using the bulk method and analyzed using in a KBr disc gave similar IR spectra, however, the spin coating method facilitated removal of solvent and moisture and was therefore the method of choice. FT-IR spectra were collected on a Bio-Rad FTS-6000 (Bio-Rad, Cambridge, MA). One hundred twenty-eight scans were collected at a resolution of 4/cm for each sample over the wavenumber region 6000–400 cm⁻¹. The optics and sample compartment were purged with dry N₂ gas to prevent

absorption of moisture into the sample and other spectral interference from water vapor. Win-IR Pro v3.3 software (Digilab, Randolph, MA) was used for the analysis of spectra.

RESULTS

Determination of Nucleation Rates from Amorphous Systems

Figure 1 shows an example of optical images obtained from a sample prepared by spin coating a solution of felodipine immediately after

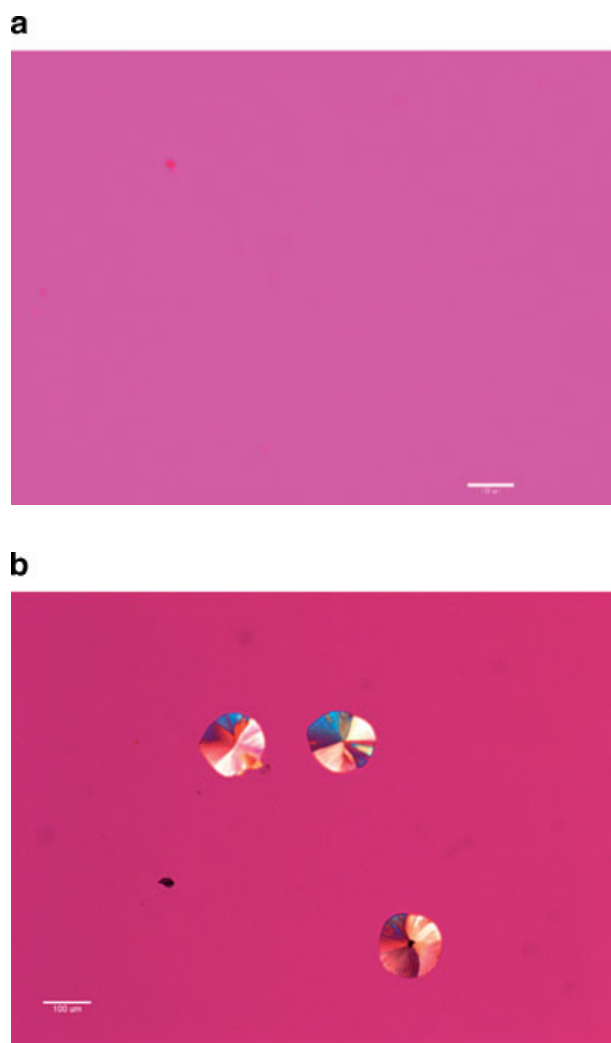


Figure 1. Photomicrograph of crystals grown at 22°C, 0% RH from amorphous felodipine prepared by spin coating. The bar in the figures represents a scale of 100 μm . (a) Just after sample preparation; (b) after storage for several days. [Color figure can be seen in the online version of this article, available on the website, www.interscience.wiley.com.]

preparation and after storage at 0% relative humidity for several days. Immediately after preparation, an optically transparent film was produced which showed an absence of birefringence when examined with an optical microscope under polarized light, indicating that an amorphous sample has been produced. With time, approximately spherical crystallites, which were birefringent under polarized light, were observed to develop in the film. Similar results were observed for all samples prepared using this technique, enabling the nucleation and crystal growth of felodipine to be investigated from a variety of drug–polymer compositions. Figure 2 compares optical images of felodipine crystallites

produced from either amorphous felodipine alone or molecularly dispersed with a polymer. As can be seen Figure 2, the crystallites grown from a molecular dispersion of felodipine with a polymer have irregular boundaries, whereas the crystallite grown from amorphous felodipine alone has a much smoother interface with the amorphous phase. In addition, dark areas can be observed on the crystallites produced from felodipine mixed with the polymers. These dispersed dark points are attributed to isolated domains of either pure polymer or a polymer rich phase,²⁹ which has undergone a phase separation from the molecular dispersion following crystallization of the drug. The irregular spherulite shape also indicates that

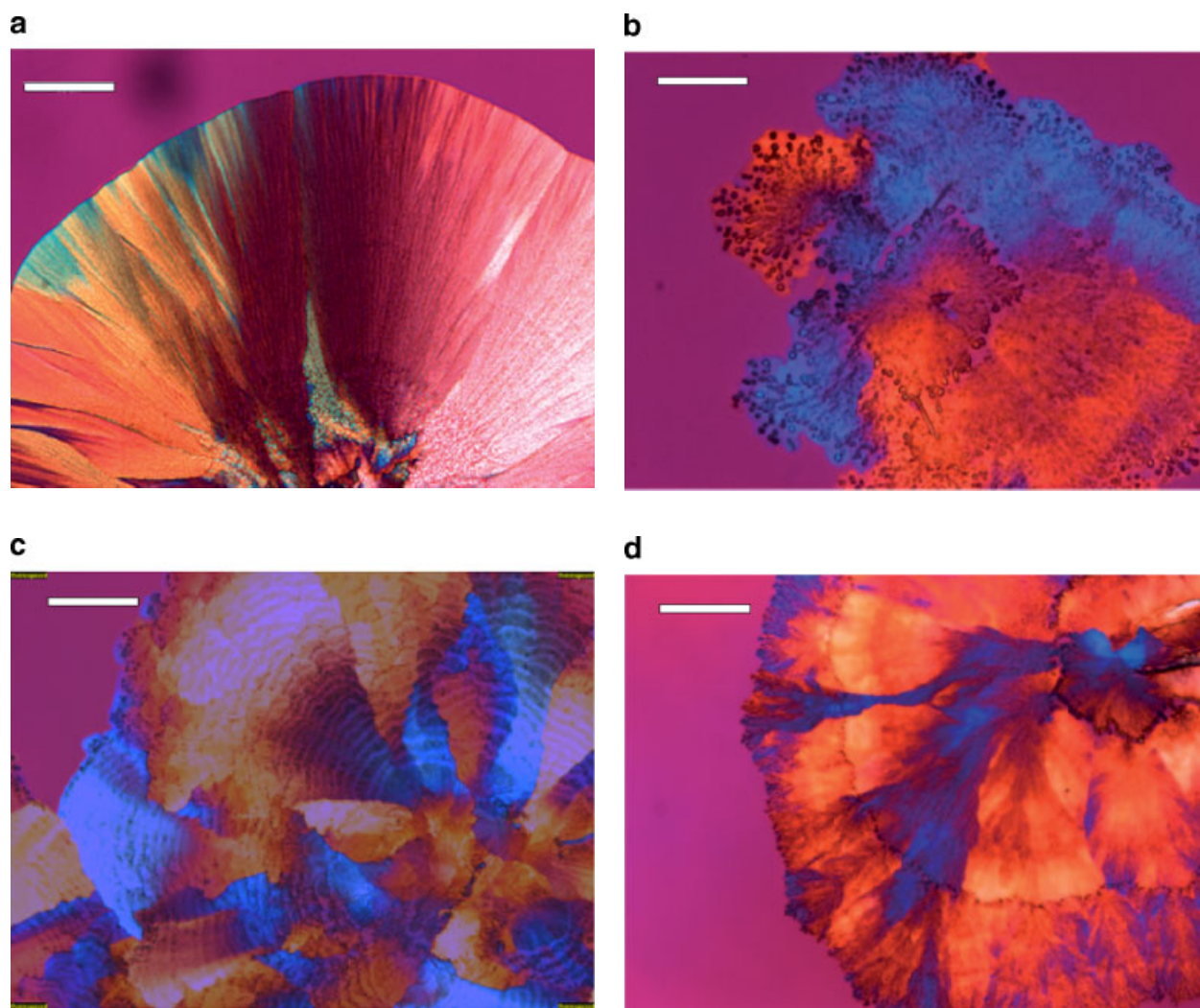


Figure 2. Photomicrographs of crystal grown from amorphous felodipine at 22°C; (a) without polymer; (b) with 3% of HPMCAS; (c) with 3% of PVP; (d) with 3% of HPMC. Bars in the figures represent the scale of 50 μm . [Color figure can be seen in the online version of this article, available on the website, www.interscience.wiley.com.]

the polymers in the solid dispersions inhibit the circular extension of crystal growth observed for pure felodipine.

Figure 3 shows an example of how the nucleation site number density per unit volume increases as a function of time for a film of felodipine stored at 0% RH. It can be seen that the number of nucleation sites increased linearly with time and thus the nucleation rate can be calculated from the slope of these data.²² The nucleation rates for felodipine alone and in solid dispersions with different polymers were obtained in this manner and are shown in Figure 4. The polymers were found to dramatically reduce nucleation rates in the amorphous solid dispersions relative to felodipine alone with a greater reduction in nucleation rate occurring with increasing polymer concentration. Thus adding only 3% w/w polymer was found to reduce the nucleation rate by around 1.5 orders of magnitude while 25% w/w polymer resulted in an approximately 2.5 orders of magnitude reduction. Interestingly, within experimental error, there was no difference in the stabilizing ability of the different polymers at any concentration.

Glass Transition Temperatures of Mixtures of Felodipine and Polymer

Analysis of mixtures using the DSC method described above revealed a single T_g event for all samples that depended on the composition and was intermediate to the T_g values of the

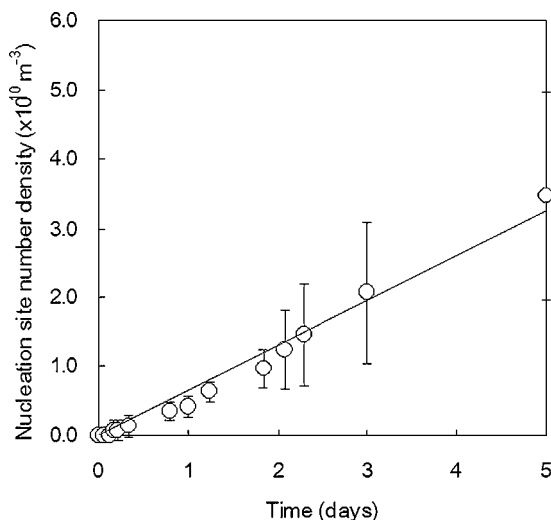


Figure 3. Nucleation site number density for crystals formed from amorphous felodipine as a function of time (22°C, 0% RH). Error bar represents standard deviation, $n = 3$. The slope of the line is the steady state nucleation rate.

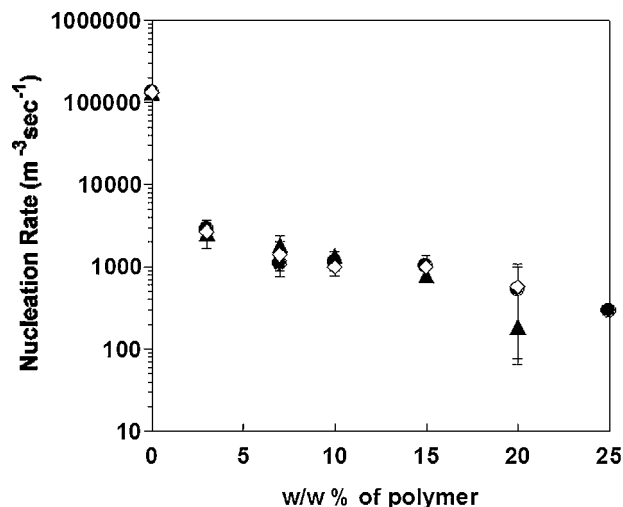


Figure 4. Nucleation rate as a function of polymer concentration. Symbols represent data for felodipine with PVP (●), HPMCAS (▲), and HPMC (◆). Error bars represents standard deviation, $n = 3$.

pure components, indicating that mixtures were miscible across the entire composition range. Figure 5 shows how T_g of the solid dispersions varies as a function of polymer composition for each polymer. In general, it can be seen that the T_g values increased with increasing additive concentration. However, from Figure 5b and c it can be seen that for HPMCAS and HPMC at low additive concentrations, the T_g values are not significantly higher than for felodipine alone and only mixtures with a polymer concentration greater than 30% w/w resulted in an increase in T_g . These results are consistent with previous observations.³⁰

The experimental T_g values of felodipine with the various polymers were compared to those predicted using the Gordon–Taylor equation. The measured T_g values of mixtures with HPMCAS and HPMC showed negative deviations from ideal behavior with the deviations being most apparent at midrange compositions, while the T_g of the mixture with PVP were quite close to predictions from the Gordon–Taylor equation. The measured T_g values were also compared with those predicted using the Couchman–Karasz equation and similar deviations as described above were observed. It has been suggested that there may be a correlation between the T_g difference of the two components used to form the dispersion and the extent of the deviation from ideality, whereby a larger difference in the T_g of the two materials will lead to larger deviations.³⁰ In this study, no such correlation was apparent.

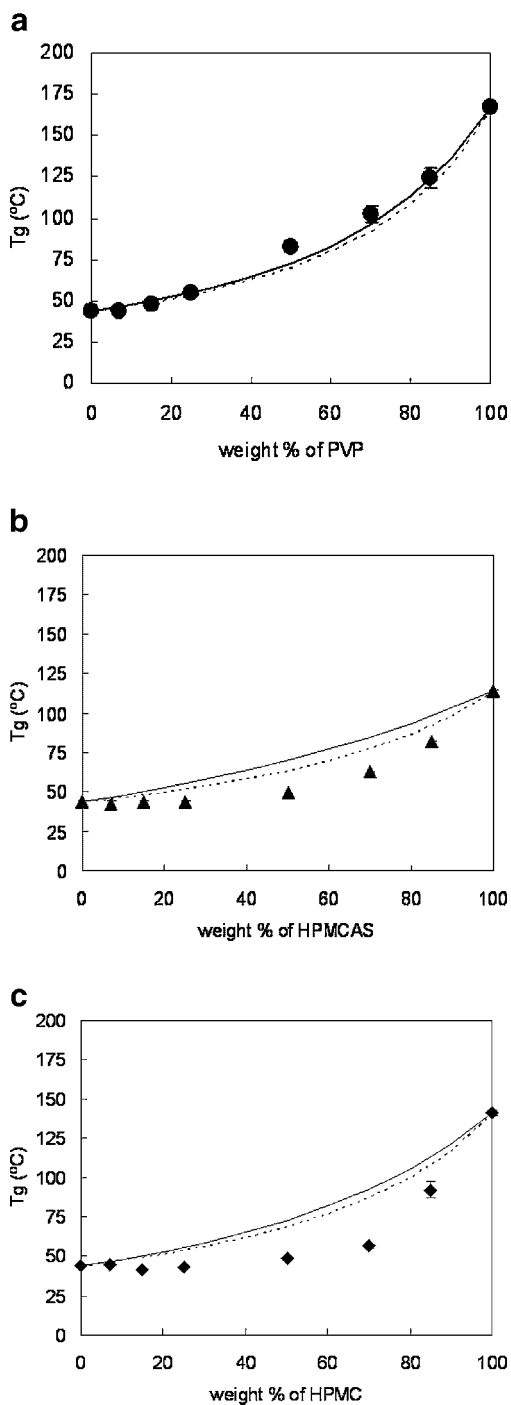


Figure 5. T_g of amorphous felodipine as a function of weight fraction polymer (a) PVP, (b) HPMCAS, and (c) HPMC. Error bars represent the standard deviation, $n = 3$. The broken line represents the fit to the Gordon–Taylor equation, the solid line represents the fit to the Couchman–Karasz equation.

Enthalpy Relaxation Measurements

τ values were calculated by fitting the enthalpy relaxation data (shown in Figure 6) using a

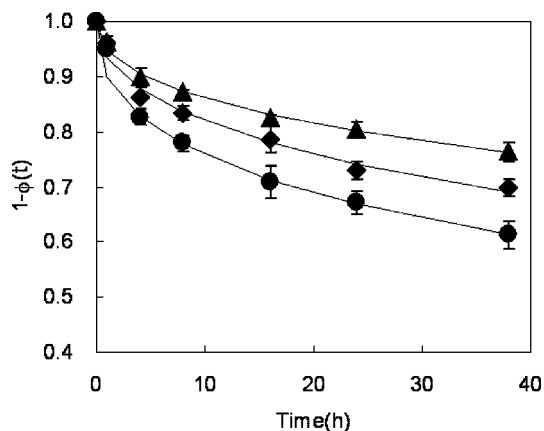


Figure 6. Enthalpy relaxation data for amorphous felodipine with PVP (9:1) (●), HPMCAS (9:1) (▲), and HPMC (9:1) (◆). Error bars represent the standard deviation ($n = 3$). The lines represent the fit to the Kohlrausch–Williams–Watts equation.

nonlinear regression method (R^2 coefficients > 0.9) τ values for solid dispersions of felodipine with PVP, HPMCAS, and HPMC were estimated as 208, 687, and 319 h, respectively, with a β values of 0.42, 0.45, and 0.47, respectively.

Spectroscopic Evidence of Intermolecular Interactions

FT-IR spectroscopy was used to examine the intermolecular interactions between felodipine and each polymer in the solid dispersions. Felodipine has an NH function that is capable of forming hydrogen bonds. Previous studies have shown that the position of the NH peak is sensitive to the strength of the hydrogen bond formed.²⁰ In crystalline felodipine, the NH group is weakly hydrogen bonded to a carbonyl function of another drug molecule.³¹ FTIR studies have also shown that in amorphous felodipine, hydrogen bonding also occurs between the NH group and the carbonyl function, but that the average hydrogen bonding is actually stronger than in the crystalline state.²⁰ Hence both the NH region of the spectrum and the carbonyl region can be used to provide information about interactions between felodipine and the polymers. Figures 7–9 show the IR spectra of the solid dispersions in (a) the NH stretching region and (b) the C=O stretching region, for samples containing between 0 and 70% polymer. Firstly it is apparent that crystalline and amorphous felodipine have very different spectra as reported previously where the NH stretch for crystalline felodipine at 3373 cm^{-1}

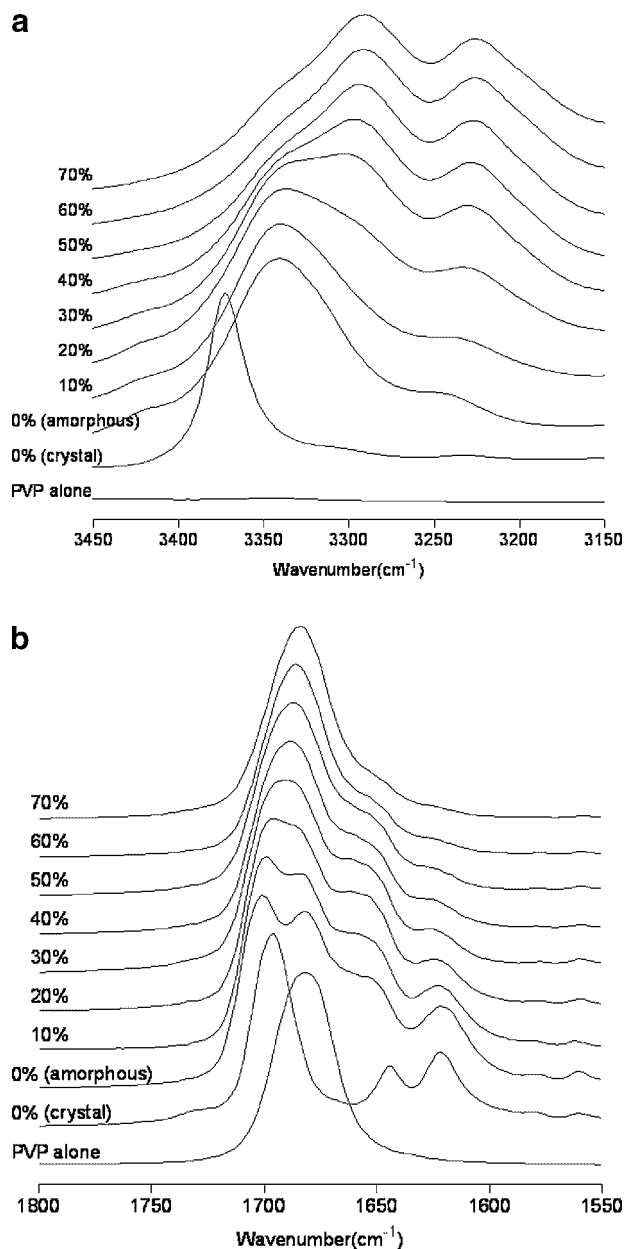


Figure 7. Infrared spectra of felodipine/PVP solid dispersion showing (a) the NH stretching region (3150–3450/cm) and (b) the carbonyl stretching region (1550–1800/cm). Percentages represent the weight percentage of PVP in the solid dispersion.

is shifted to 3341 cm^{-1} in the amorphous material and the single C=O stretching vibration seen in the crystalline sample at 1696 cm^{-1} , splits into two peaks at 1701 and 1682 cm^{-1} ; these peaks have been previously assigned to nonhydrogen bonded and hydrogen bonded carbonyl, respectively.²⁰ In order to understand how the polymers interact with felodipine in the solid dispersions, it is necessary to examine changes between the

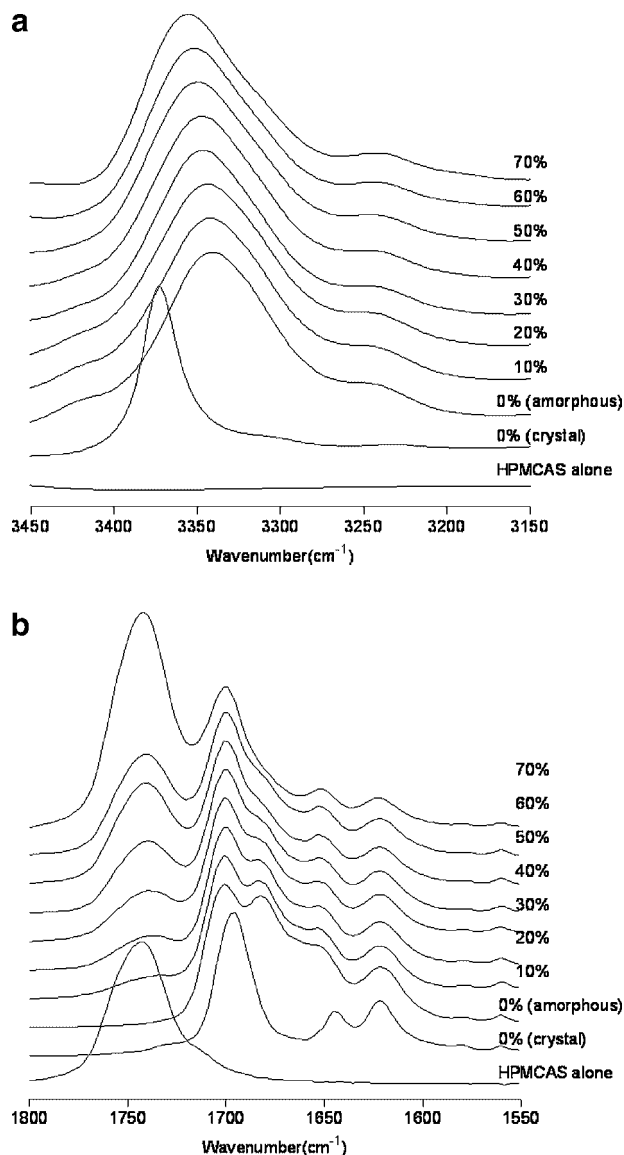


Figure 8. Infrared spectra of felodipine/HPMCAS solid dispersion showing (a) the NH stretching region (3150–3450/cm) and (b) the carbonyl stretching region (1550–1800/cm). Percentages represent the weight percentage of HPMCAS in the solid dispersion.

spectrum of pure amorphous felodipine and that of felodipine in the presence of the polymers.

The NH stretching region for felodipine in solid dispersions with HPMCAS is shown in Figure 8a. It can be seen that as the concentration of HPMCAS increases, the NH stretching peak of felodipine broadens and develops a shoulder on the low wavenumber side. This is most apparent for the solid dispersion containing 30% HPMCAS where a broad peak, which appears to be composed of two poorly resolved peaks with maxima at approximately 3345 and

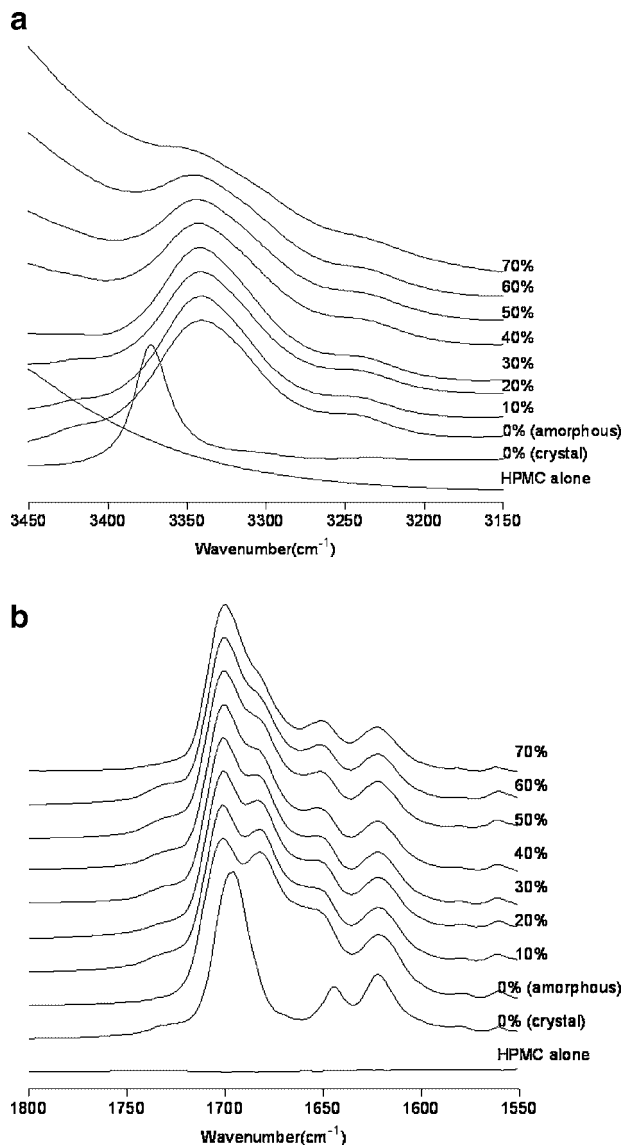


Figure 9. Infrared spectra of felodipine/HPMC solid dispersion showing (a) the NH stretching region (3150–3450/cm) and (b) the carbonyl stretching region (1550–1800/cm). Percentages represent the weight percentage of PVP in the solid dispersion.

3290/cm, is present. As the concentration of PVP is further increased, the low wavenumber shoulder increases in intensity at the expense of the high wavenumber peak. The downward shift in position of the NH peak indicates that stronger hydrogen bonds are formed between the drug and polymer relative to those present in amorphous felodipine.³² However, it should be noted that in all the solid dispersions, there appears to be two populations of felodipine molecules present, those interacting with other drug molecules and those

interacting with PVP. Hence, even at a level of 70% PVP, a shoulder is still present at 3345/cm which is indicative of amorphous drug–drug interactions. In contrast to the PVP solid dispersions, the felodipine NH peak undergoes a slight increase to a higher wavenumber with HPMCAS indicating that interactions formed between felodipine and HPMCAS are slightly weaker than in amorphous felodipine (Fig. 8a). For HPMC, the NH peak position stays in essentially the same position as in amorphous felodipine but broadens slightly (Fig. 9a). In this case, there are two possible interpretations; the NH peak position is unchanged because there is no interaction between felodipine and HPMC or it is unchanged because the strength of the interaction is comparable that found in amorphous felodipine alone. If the former situation was occurring, then no change would be expected for the carbonyl peaks of felodipine. However, it was observed for solid dispersions of both HPMCAS and HPMC, that the height of the 1701/cm nonhydrogen bonded carbonyl peak increased relative to the hydrogen bonded carbonyl peak at 1682/cm. This is shown graphically in Figure 10 where it can be seen that the peak height ratio increases with the polymer concentration in the solid dispersion. The increase in the peak intensity of free C=O groups (1701/cm) strongly suggests that the hydrogen bonding between NH groups and C=O groups in amorphous felodipine is disrupted by a new interaction formed between the NH groups of felodipine and some acceptor group (see Table 1)

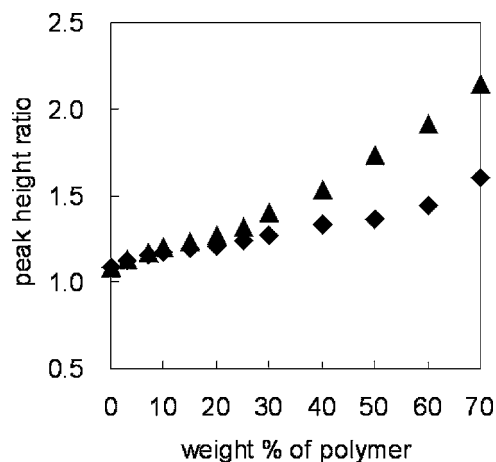


Figure 10. Peak height ratio of nonhydrogen bonded carbonyl peak (1701/cm) relative to hydrogen bonded carbonyl peak (1682/cm). Symbols represent data for felodipine with HPMCAS (▲) and HPMC (◆).

present in HPMCAS and HPMC with the extent of the interaction increasing with increasing polymer content. For PVP, no such clear-cut changes could be detected due to interference in this spectral region from the intense PVP carbonyl peak (Fig. 7b). A summary of NH peak positions for amorphous felodipine and felodipine in the solid dispersions is shown in Table 2.

DISCUSSION

The results of this study clearly show that the three polymers investigated inhibit crystallization of amorphous felodipine by reducing the nucleation rate. Crystallization inhibition of an amorphous drug through the formation of a molecular dispersion with a polymer is a well-known phenomenon, however, the mechanisms by which such polymers affect crystallization are less clear. Several potential mechanisms have been suggested including: increasing the glass transition temperature (antiplasticization) and reduction of molecular mobility, disruption of critical drug–drug interactions and the formation of drug–polymer interactions.^{14–20} Reviewing the pharmaceutical literature in this area reveals that there is a lack of consensus regarding the dominant mechanism. Van den Mooter et al.¹⁵ have emphasized the importance of the increase in T_g (antiplasticization) for the solid dispersion relative to that of the drug alone. However, Matsumoto and Zografi³³ observed a significant inhibition of indomethacin crystallization at levels of PVP that were too low to increase the T_g of the system and concluded that polymers can exert an inhibitory effect on crystallization even if the T_g of the system is not increased. Further support for this conclusion is provided by the work of Khougaz and Clas³⁴ who reported that the tendency for an amorphous drug to crystallize

was reduced when molecularly dispersed with a polymer even when the T_g of the solid dispersion was lower than that of the drug alone. In this study, it was observed that each of the three polymers used was equally effective at reducing the nucleation of felodipine for all compositions between 0 and 25% w/w. However, the T_g s of the pure dry polymers are quite different; the T_g of PVP was 167°C, HPMC was 140°C, and HPMCAS had a T_g of 114°C. Therefore, the extent of antiplasticization of the dry solid dispersions is different as seen from Figure 5. PVP acts as the best antiplasticizing agent increasing the T_g of the solid dispersion relative to pure felodipine, at all concentrations. However, due to nonidealities, neither HPMC nor HPMCAS result in an elevation of T_g for the 0–25% w/w concentration range relevant to the nucleation studies. The T_g in these latter systems is identical to that of pure felodipine, whereas for PVP it is raised by 10°C at a 25% polymer level. Two observations can, therefore, be made, (i) an increase in T_g relative to that of the pure drug was not required to decrease the nucleation rate, in agreement with previous studies, and (ii) there was no correlation between the T_g of the system (approximately 10°C variation) and the nucleation rate. While it would be anticipated that an increase in T_g for the system would certainly contribute to crystallization inhibition, these results suggest that it is not the only factor influencing the physical stability of solid dispersions.

Interactions between drug and polymer are also thought to be important,^{19–21} although it has also been argued that they are not necessary for stabilization.¹⁵ Intermolecular interactions can be arbitrarily divided into two categories, non-specific interactions such as van der Waals forces and specific interactions such as hydrogen bonds³⁵ and to achieve molecular level miscibility (i.e., a one phase system), there must be some level of hetero (or adhesive) interactions between the two molecular species in the system. Specific interactions (hydrogen bonding and ion–dipole interactions) have been observed in several pharmaceutical solid dispersions.^{19–21} Since some level of hetero interactions is a prerequisite for the formation of a single phase system, the specific role of drug–polymer interactions in crystallization inhibition is somewhat hard to evaluate although there is some evidence indicating that they are of importance. For example, Aso et al.³⁶ showed that the molecular mobility of sucrose was altered in the presence of PVP as a result of a specific hetero

Table 2. NH Peak Position in Amorphous Felodipine and Solid Dispersions

H bond pattern	Peak position (cm ⁻¹)
Felodipine–felodipine	3340
Felodipine–PVP	3290
Felodipine–HPMCAS	3356
Felodipine–HPMC	3344

For the solid dispersions, the peak position was taken from samples containing 70% w/w polymer.

interaction which effectively coupled the motion of the two molecules. In another study, the crystallization tendency of a series of benzodiazepines with different functional groups was investigated and it was found that only the compound capable of forming a hydrogen bond with the carrier (a phospholipid) showed no crystallization.³⁷ In our studies, the order of the felodipine-polymer hydrogen bonding strength was found to be PVP > HPMC > HPMCAS. However, it should also be noted that not all of the felodipine NH groups hydrogen bonded with the polymer and no comment can be made about the extent of the drug-polymer interactions (it was not possible to extract such quantitative interactions from our spectroscopic data). Hydrogen bonding interactions between PVP and felodipine were stronger than in pure amorphous felodipine, whereas in HPMC, the interaction was of a similar strength to amorphous felodipine and slightly weaker in solid dispersions with HPMCAS. Thus it is clear that although the strength of the drug-polymer interaction varies, there is no correlation with the effect of the polymer on the nucleation rate. These results differ from those of Miyazaki et al.²¹ who found that polyacrylic acid was a better inhibitor of acetaminophen crystallization than PVP (although the T_g s were the same for both systems) and attributed the enhanced stabilizing ability to the formation of stronger drug-polymer interactions in the former system.

From an analysis of T_g as a function of polymer concentration, solid dispersions with the cellulosic polymers show nonideal mixing as reflected by the negative deviations from the Gordon-Taylor and the Couchman-Karasz equations. It has been reported that when the interactions between like molecular species are greater in number and/or strength relative to the interactions between unlike molecular species, the mixture has a lower T_g than an ideally mixed system.³⁸ The results of this study, therefore, suggest that the sum of interaction energy between felodipine and HPMCAS or HPMC is lower than the sum of the drug-drug and polymer-polymer energies. This is not the case for the PVP-felodipine system which shows more ideal mixing behavior. These results are supported by the spectroscopic data which indicate that the interactions are weakest in the drug-polymer system that shows the greatest negative deviations from ideality.

To attempt to explain the similar magnitude of nucleation rate reduction by the polymers, it is relevant to discuss the factors governing the

nucleation rate. Three factors can be considered as important, namely the thermodynamic driving force, the kinetic barrier and the molecular recognition events necessary to form the nucleus. The first two factors can be described using classic homogeneous nucleation theory for condensed systems (although it should be noted that nucleation is most likely heterogeneous in our systems). An expression for the nucleation rate can be written in terms of a thermodynamic barrier to nucleation G^* and a kinetic barrier G_a .³⁹

$$I = A \exp \frac{-(\Delta G^* + \Delta G_a)}{kT} \quad (8)$$

Where k is Boltzmann's constant and T is given in Kelvin. A is a constant. ΔG^* is the local free energy change associated with the formation of a region of a new phase in the parent phase and is related to energy required to form the new interface (ΔG_s) and the bulk free energy difference between the amorphous and crystalline phase (ΔG_v). ΔG_s is unfavorable to nucleation since energy is required to create a new interface while ΔG_v is favorable since the free energy of the crystalline phase is lower than that of the amorphous phase. ΔG_a is the activation energy associated with the crossing of the liquid-solid interface and has been related to diffusivity or reciprocal viscosity.

The formation of a solid dispersion can potentially influence both ΔG^* and ΔG_a . In a molecular mixture of drug and polymer, the term ΔG_v will be reduced in magnitude and the driving force for nucleation reduced. This is because the free energy of the drug in the mixture will be lower relative to the pure liquid phase, while the free energy of the crystalline phase will be unchanged.⁴⁰ The reduced free energy of felodipine in the mixture arises because of the mixing entropy and any specific drug-polymer interactions that result in a negative heat of mixing. For a polymer-small molecule system, the activity of the small molecule in the mixture can be described by the Flory-Huggins equation:⁴¹

$$\ln a = \ln \Phi_1 + \left(1 - \frac{1}{x_{12}}\right) \Phi_2 + \chi \Phi_2^2 \quad (9)$$

Where a is the activity of component 1 (drug) and Φ is the volume fraction of components 1 and 2 (polymer). x_{12} is the relative molecular volume and χ is known as the Flory-Huggins parameter. The χ parameter is a measure of compatibility between the two components and reflects the

nonideality of mixing for the system. The first two terms represent the entropy of mixing. Based on literature data for reasonably comparable systems (PVP and sucrose or water),^{42,43} the Flory–Huggins equation would only predict a significant lowering of the small molecule activity when the volume fraction of the polymer approaches a value greater than 0.5. If the activity of the drug in the solid dispersion is relatively unchanged then the ΔG_v term will not be significantly reduced over the range of polymer concentrations used in these studies and hence probably cannot account for the observed reduction in nucleation rate.

In Equation 8, ΔG_a is generally described as the free energy of activation for the short-range diffusion of molecules moving across an interface to join a new lattice.³⁹ The polymer can potentially affect drug diffusion via several mechanisms. These would include as a diluent,^{39,44} through specific interactions with the drug, and through accumulation at the nucleus-amorphous matrix interface. If the polymer was only acting as a diluent, then the nucleation rate would be expected to vary directly with the volume fraction of polymer.^{39,44} This is clearly not the case, as can be seen from Figure 9, where adding 3% polymer has a large effect on the nucleation rate. Specific interactions might be expected to reduce the diffusivity of the drug through coupling the motion of the drug to the polymer. However, this parameter is hard to assess as different populations of drug molecules will exist in the solid dispersion; those interacting with the polymer and those interacting with other drug molecules. Polymer accumulation at the growing crystal front is a phenomenon that has been discussed in the polymer literature and is a potentially relevant mechanism for the solid dispersion systems.⁴⁵ In the case of a miscible drug–polymer blend, it is unlikely that the polymer would be incorporated into the crystal lattice when the drug crystallizes, hence rejection of the polymer will occur and the polymer must diffuse into the surrounding amorphous phase. Polymer accumulation at the crystal-amorphous interface can arise if diffusion of the polymer away from the interface is slow, as would be expected at temperatures below T_g . Such a polymer rich layer would impede transport of drug to the crystal since the local concentration of drug will be decreased and molecular mobility in this localized region will be reduced due to an increase in T_g . The presence of a polymer rich layer may also increase the energy penalty for creating new

surface (i.e., change the ΔG_s term of Equation (8)). A polymer accumulation mechanism has been proposed previously to explain why the extent of crystallization in solid dispersions of indomethacin with low concentrations of PVP varied with particle size.⁴⁶ Based on these considerations, it seems reasonable to speculate that the polymers result in an increase in magnitude of the ΔG_a term in Equation 8 with a consequent decrease in nucleation and growth rates. Furthermore, it appears that after the initial large decrease in nucleation rate with a small amount of polymer, the effect of the polymer on the ΔG_a term is related to the amount of polymer added and, for the three polymers investigated, is relatively independent of the polymer type. These observations are consistent with the polymers acting as a physical impediment to nucleation (through reducing the mass transport of drug) at the nucleus-matrix interface, whereby the volume fraction of the polymer is the controlling parameter. Some evidence for this mechanism is provided by Figure 2 where it can be seen that the uniform spherulitic growth observed for felodipine alone is disrupted by the polymers. Furthermore, small “droplets” are present on the crystallites. These droplets form ring-like patterns and are also present at the edges of the crystals (this can be most clearly seen in Fig. 2b). It is thought that these droplets represent a polymer rich phase. Clearly this observation requires further investigation.

CONCLUSIONS

In the absence of moisture, three chemically different polymers, PVP, HPMC, and HPMCAS were found to be equally effective at decreasing the nucleation rate of felodipine from amorphous solid dispersions at a given weight percentage of polymer. No correlation between nucleation rate and the glass transition temperature of the pure polymer, the glass transition temperature of the solid dispersion or the strength of the drug–polymer hydrogen bonding interactions could be made. It was speculated that the polymeric additives affect nucleation kinetics by increasing the kinetic barrier to nucleation with the scale of the effect being related to the polymer concentration and, for the three specific polymers studied, independent of the polymer physiochemical properties.

ACKNOWLEDGMENTS

Professor George Zografi is thanked for many enlightening discussions about this research. The authors are grateful to Dr Sheri L. Shamblin for helpful comments regarding this work. LST thanks AFPE/AACP for a New Investigator Award. HK acknowledges Astellas Pharma, Inc. for granting him a leave of absence to undertake this work.

REFERENCES

1. Sekiguchi K, Obi N. 1961. Studies on absorption of eutectic mixture 1. A comparison of the behavior of eutectic mixture of sulphathiazole and that of ordinary sulfathiazole in man. *Chem Pharm Bull* 9:866–872.
2. Chiou WL, Riegelman S. 1971. Pharmaceutical applications of solid dispersions. *J Pharm Sci* 60:1281–1302.
3. Ford JL. 1986. The current status of solid dispersions. *Pharm Acta Helv* 61:69–88.
4. Serajuddin ATM. 1999. Solid dispersions of poorly water-soluble drugs: Early promises, subsequent problems and recent breakthroughs. *J Pharm Sci* 88:1058–1066.
5. Leuner C, Dressman J. 2000. Improving drug solubility for oral delivery using solid dispersions. *Eur J Pharm Biopharm* 50:47–60.
6. Simonelli AP, Mehta SC, Higuchi WI. 1970. Inhibition of sulfathiazole crystal growth by PVP. *J Pharm Sci* 59:633–637.
7. Yoshioka M, Hancock BC, Zografi G. 1995. Inhibition of indomethacin crystallization in poly(vinylpyrrolidone). *J Pharm Sci* 84:983–986.
8. Taylor LS, Zografi G. 1997. Spectroscopic characterization of interactions between PVP and indomethacin in amorphous molecular dispersions. *Pharm Res* 14:1691–1698.
9. Chou WL, Riegelman S. 1969. Preparation and dissolution characteristics of several-fast release solid dispersions of griseofluvin. *J Pharm Sci* 58:1505–1509.
10. Lin CW, Cham TM. 1996. Effect of particle size on the available surface area of nifedipine from nifedipine-poly(ethylene glycol) 6000 solid dispersions. *Int J Pharm* 127:261–272.
11. Mura P, Manderioli A, Bramanti G, Ceccarelli L. 1996. Properties of solid dispersion of naproxen in various poly(ethylene glycol)s. *Drug Dev Ind Pharm* 22:909–916.
12. Hino T, Ford JL. 2001. Characterization of the hydroxypropylmethylcellulose-nicotinamide binary system. *Int J Pharm* 219:39–49.
13. Yamashita K, Nakate T, Okimoto K, Ohike A, Tokunaga Y, Ibuki R, Higaki K, Kimura T. 2003. Establishment of new preparation method for solid dispersion formulation of tacrolimus. *Int J Pharm* 267:79–91.
14. Jolley JE. 1970. Microstructure of photographic gelatin binders. *Photogr Sci Eng* 14:169–177.
15. Van den Mooter G, Wuyts M, Bleton N, Busson R, Grobet P, Augustijns P, Kinget R. 2001. Physical stabilisation of amorphous ketoconazole in solid dispersions with polyvinylpyrrolidone K25. *Eur J Pharm Sci* 12:261–269.
16. Oksanen CA, Zografi G. 1990. The relationship between the glass transition temperature and water vapor absorption by poly(vinylpyrrolidone). *Pharm Res* 7:654–657.
17. Abe Y, Arahori T, Naruse A. 1976. Crystallization of calcium metaphosphate glass below the glass transition temperature. *A J Am Ceram Soc* 59:487–490.
18. Yoshioka M, Hancock BC, Zografi G. 1994. Crystallization of indomethacin from the amorphous state below and above its glass transition temperature. *J Pharm Sci* 83:1700–1705.
19. Taylor LS, Zografi G. 1997. Spectroscopic characterization of interactions between PVP and indomethacin in amorphous molecular dispersions. *Pharm Res* 14:1691–1698.
20. Tang XC, Pikal MJ, Taylor LS. 2002. A spectroscopic investigation of hydrogen bond patterns in crystalline and amorphous phases in dihydropyridine calcium channel blockers. *Pharm Res* 19:477–483.
21. Miyazaki T, Yoshioka S, Aso Y, Kojima S. 2004. Ability of polyvinylpyrrolidone and polyacrylic acid to inhibit the crystallization of amorphous acetaminophen. *J Pharm Sci* 93:2710–2717.
22. Andronis V, Zografi G. 2000. Crystal nucleation and growth of indomethacin polymorphs from the amorphous state. *J Non-Cryst Sol* 271:236–248.
23. Inoue S, Oldenbourg R. 1995. Microscopes. In: Bass M, editor. *Handbook of optics*, Vol. 2. New York: McGraw-Hill.
24. Gordon M, Taylor JS. 1952. Ideal co-polymers and the second-order transitions of synthetic rubbers. *J Appl Chem* 2:493–500.
25. Simha R, Boyer RF. 1962. On a general relation involving the glass temperature and coefficients of expansion of polymers. *J Chem Phys* 37:1003–1007.
26. Couchman PR, Karasz FE. 1978. A classical thermodynamic discussion on the effect of composition on glass-transition temperatures. *Macromolecules* 11:117–119.
27. Hancock BC, Shamblin SL, Zografi G. 1995. Molecular mobility of amorphous pharmaceutical solids below their glass transition temperatures. *Pharm Res* 12:799–806.

28. Shamblin SL, Zografi G. 1998. Enthalpy relaxation in binary amorphous mixtures containing sucrose. *Pharm Res* 15:1828–1834.
29. Nitta K, Shin Y, Hashiguchi H, Tanimoto S, Terano M. 2005. Morphology and mechanical properties in the binary blends of isotactic polypropylene and novel propylene-co-olefin random copolymers with isotactic propylene sequence 1. Ethylene-propylene copolymers. *Polymer* 46:965–975.
30. Shamblin SL, Taylor LS, Zografi G. 1998. Mixing behavior of colyophilized binary systems. *J Pharm Sci* 87:694–701.
31. Fossheim R. 1986. Crystal structure of the dihydro-pyridine Ca²⁺ antagonist felodipine. Dihydro-pyridine binding prerequisites assessed from crystallographic data. *J Med Chem* 29:305–307.
32. Jeffrey GA. 1997. An introduction to hydrogen bonding. New York: Oxford University Press.
33. Matsumoto T, Zografi G. 1999. Physical properties of solid dispersions of indomethacin with poly(vinylpyrrolidone) and poly(vinylpyrrolidone-co-vinyl acetate) in relation to indomethacin crystallization. *Pharm Res* 16:1722–1728.
34. Khougaz K, Clas SD. 2000. Crystallization inhibition in solid dispersions of MK-0591 and poly(vinylpyrrolidone) polymers. *J Pharm Sci* 89: 1325–1334.
35. Coleman MM, Graf JF, Painter P, 1991. Specific interactions and the miscibility of polymer blends. Lancaster: Technomic Publishing Company, Inc.
36. Aso Y, Yoshioka S, Chang J, Zografi G. 2002. Effect of water on the molecular mobility of sucrose and poly(vinylpyrrolidone) in a colyophilized formulation as measured by C-13-NMR relaxation time. *Chem Pharm Bull* 50:822–826.
37. Fujii M, Hasegawa J, Kitajima H, Matsumoto M. 1991. The solid dispersion of benzodiazepins with phosphatidylcholine—the effect of substituents of benzodiazepins on the formation of solid dispersions. *Chem Pharm Bull* 39:3013–3017.
38. Brekner MJ, Schneider HA, Cantow HJ. 1988. Approach to the composition dependence of the glass transition temperature of compatible polymer blends: 1. *Polymer* 29:78–85.
39. Turnbull D, Fisher JC. 1949. Rate of nucleation in condensed systems. *J Chem Phys* 17:71–73.
40. Angell CA. Origin and control of low-melting behavior in salts, polysalts, salt solvates, and glass formers. In: Gaune-Escard, editor. 2002. *Molten salts: From fundamentals to applications*. The Netherlands: Kluwer Academic Publishers, pp 305–322.
41. Flory PJ. 1953. *Principles of polymer chemistry*. Ithaca, New York: Cornell University.
42. Hancock BC, Zografi G. 1993. The use of solution theories for predicting water vapor absorption by amorphous pharmaceutical solids: A test of the Flory-Huggins and Vrentas models. *Pharm Res* 10:1262–1267.
43. Zhang J, Zografi G. 2001. Water vapor absorption into amorphous sucrose-poly(vinylpyrrolidone) and trehalose-poly(vinylpyrrolidone) mixtures. *J Pharm Sci* 90:1375–1385.
44. Chang LQ, Shepherd D, Sun J, Ouellette D, Grant KL, Tang XC, Pikal MJ. 2005. Mechanism of protein stabilization by sugars during freeze-drying and storage: Native structure preservation, specific interaction, and/or immobilization in a glassy matrix? *J Pharm Sci* 94:1427–1444.
45. Stein RS. 1994. Crystallization from polymer blends. *Materials Research Society Symposium Proceedings* 321 (Crystallization and Related Phenomena in Amorphous Materials). pp 531–542.
46. Crowley KJ, Zografi G. 2003. The effect of low concentrations of molecularly dispersed poly(vinylpyrrolidone) on indomethacin crystallization from the amorphous state. *Pharm Res* 20:1417–1422.